PRAMANA
— journal of
physics

Vol. 67, No. 6
December 2006
pp. 1055–1071

Does the classically chaotic Henon–Heiles oscillator exhibit quantum chaos under intense laser fields?

NEETU GUPTA[1] and B M DEB[2,*]
[1]Theoretical Chemistry Group, Department of Chemistry, Panjab University, Chandigarh 160 014, India
[2]S.N. Bose National Centre for Basic Sciences, JD Block, Sector-III, Salt Lake, Kolkata 700 098, India and Jawaharlal Nehru Centre for Advanced Scientific Research, Jakkur, Bangalore 560 064, India
E-mail: bmdeb@yahoo.co.in; bidyendu@bose.res.in
*Corresponding author.

MS received 30 January 2006; revised 25 July 2006; accepted 22 August 2006

Abstract. The quantum dynamics of an electron moving under the Henon–Heiles (HH) potential in the presence of external time-dependent (TD) laser fields of varying intensities have been studied by evolving in real time the unperturbed ground-state wave function $\psi(x, y, t)$ of the HH oscillator. The TD Schrödinger equation is solved numerically and the system is allowed to generate its own wave packet. Two kinds of sensitivities, namely, sensitivity to the initial quantum state and to the Hamiltonian, are examined. The threshold intensity of the laser field for an electron moving in the HH potential to reach its continuum is identified and in this region quantum chaos has been diagnosed through a combination of various dynamical signatures such as the autocorrelation function, quantum 'phase-space' volume, 'phase-space' trajectory, distance function and overlap integral (akin to quantum fidelity or Loschmidt echo), in terms of the sensitivity towards an initial state characterized by a mixture of quantum states (wave packet) brought about by small changes in the Hamiltonian, rather than a 'pure' quantum state (a single eigenstate). The similarity between the HH potential and atoms/molecules in intense laser fields is also analyzed.

Keywords. Quantum chaos; coupled oscillators; multiphoton processes; high-order harmonics generation.

PACS Nos 05.45.Mt; 05.45.Xt; 42.50.Hz; 42.65.Ky

1. Introduction

During the last three decades the quantum domain behaviour of the fascinating and classically chaotic Henon–Heiles oscillator (HHO) [1] has been studied in considerable detail [2–13]. The quantum HHO has a dissociation energy of 13.3333 a.u. and 99 bound states [14]; some of the bound-state energy levels are doubly degenerate [5]. The regime of stochastic motion sets in at around $E = 9.0$, which

is about two-thirds of the well-depth of the dissociation limit; approximately half of the bound states are in this regime, i.e., between $E = 9.0$ and the dissociation limit [13,14]. In studying the possibility of quantum chaos for a classically chaotic system, earlier efforts were mainly directed towards evolving an external Gaussian wave packet under the HH potential by numerically solving the time-dependent Schrödinger equation (TDSE) wherein the Hamiltonian was time-independent [7–12].

In contrast to a classically chaotic system, where the exponential divergence of trajectories in phase-space is an unambiguous and confirmatory signature of chaos [15–17], the decision about whether a quantum system is chaotic or not is frequently not unambiguous and one cannot generally depend on only one 'signature' of quantum chaos. This is mainly because the deterministic concept of an orbit or a trajectory in classical mechanics vanishes in quantum mechanics. The difficulty is further compounded by the fact that in quantum domain, classical chaos might vanish due to quantum fluctuations although this need not be universally true (see the argument in [18]).

In spite of previous extensive works, the question whether the classically chaotic HHO can exhibit quantum chaos under a time-dependent Hamiltonian does not seem to have been addressed so far. In this paper, we pursue this question by taking the TD potential as arising from an intense laser field acting on an electron moving as an HHO, without employing an external wave packet. The reasons for this are the following which also emphasize the importance of this problem:

(i) Atoms, molecules, clusters and solids reveal highly interesting nonlinear phenomena under intense laser fields, e.g., high-order harmonics generation (HHG), above-threshold ionization (ATI), stabilization under superintense laser fields, etc. During the last two decades, these aspects have been extensively studied both theoretically and experimentally [19–24].

(ii) It has been speculated earlier that helium atom might exhibit quantum chaos under intense laser fields [25].

(iii) Where response to intense laser fields is concerned, e.g. HHG, ATI and stabilization, a striking parallelism has been established between atoms and molecules on the one hand and one-dimensional nonlinear oscillators (with or without infinite barriers) on the other (see [26,27] and other references therein). Note that the HHO is a coupled two-dimensional system and the same parallelism should remain valid here.

(iv) An intense laser field excites an electron in an atom to the continuum. Since the HHO is classically chaotic, it might manifest quantum chaos on excitation to the continuum.

(v) Instead of evolving an external wave packet under the TDSE, it might be preferable to let the system itself (HHO in an intense laser field) generate its own wave packet which would continue to evolve under the strong TD perturbation.

In this paper, we would consider quantum chaos to be characterized by sensitive dependence on initial conditions, like classical chaos. Since the quantum time-evolution operator is unitary, this sensitivity is not towards an initial 'pure' quantum state (a single eigenstate) but towards an initial state characterized by a

mixture of quantum states (see (v) above). Therefore, our approach to study the motion of an electron under the HH potential in an intense laser field is as follows:

(a) We first calculate the ground state energy of the unperturbed HHO by numerically solving the TDSE in imaginary time. The first and second excited states are also calculated. Apart from settling the question of accuracy (see later) of our numerical algorithm for TDSE, it may be noted that the ground state is the solution at zero time (initial input) for the real-time Schrödinger equation involving the laser field. Note that our initial system of reference is the classical HHO at zero time and not the classical HHO + intense laser system.

(b) Two slightly different initial inputs are generated in two different ways: (1) Keeping the Hamiltonian the same, the ground state is obtained under two different prescribed tolerances (convergence conditions). This leads to two slightly different ground state energies and wave functions. This approach may be regarded as an 'internal' perturbation without perturbing the Hamiltonian. (2) Keeping the tolerance the same, two slightly different laser fields, i.e. Hamiltonians, are taken. The initial input at $t = 0$ (unperturbed ground state) is the same for both the Hamiltonians. But after the first time step, i.e., after $t = 0.05$ a.u., the same input state is now slightly different for the two Hamiltonians involving slightly different laser intensities.

(c) With respect to such different initial inputs, the TDSE was numerically solved in real time for lasers of varying intensities. Thus, the system generates its own wave packet. Finally, we examine a combination of several dynamical signatures of quantum chaos, viz., autocorrelation function, quantum 'phase-space' volume, quantum 'phase-space' trajectory, distance function and decay of overlap integral (similar to quantum fidelity or Loschmidt echo [28–32] which has been connected to a Lyapunov regime in some cases [32]) that have emerged over the years. Such a combination of time-dependent signatures of quantum chaos under an intense perturbation does not appear to have been tried before.

The method of calculation is described in §2. Section 3 discusses the results while §4 summarizes the conclusions.

2. Methodology

The two-dimensional TDSE is (atomic units employed unless mentioned otherwise)

$$H\psi(x, y, t) = i\frac{\partial\psi(x, y, t)}{\partial t}. \tag{1}$$

The Hamiltonian for an electron moving under the HH potential in the presence of an laser field in x-direction is given by

$$H = -\frac{1}{2}\frac{\partial^2}{\partial x^2} - \frac{1}{2}\frac{\partial^2}{\partial y^2} + V(x, y) - x\varepsilon_0 f(t)\sin(\omega_{\mathrm{L}}t), \tag{2}$$

where $\omega_{\rm L}$ is the laser frequency, $f(t)$ is the ramp function (see later), ε_0 is the peak electric field obtained from the laser intensity $I(\varepsilon_0 = (8\pi I/c)^{1/2}$ and c is the velocity of light). $V(x, y)$ is the HH potential which is given as

$$V(x,y) = \frac{1}{2}(x^2 + y^2) + \lambda x\left(y^2 - \frac{x^2}{3}\right). \tag{3}$$

Here, the coupling constant λ is taken as 0.11180340 [1–14] for the classically chaotic HH oscillator. The ground-state wave function of unperturbed HH potential is obtained by numerically solving the TDSE in imaginary time. The method is based on transforming the TDSE into an equation that resembles a diffusion quantum Monte Carlo (DQMC) equation [33]. Successive higher energies are calculated by employing the same imaginary time evolution but additionally requiring that an excited state is orthogonal to all the lower states. The numerical method reported earlier for one-dimensional oscillators [34,35] has been adopted for two-dimensional oscillators. Our calculated ground and the first two excited-state energies are in excellent agreement with the corresponding literature values (given in parentheses) [14]: $E_0 = 0.998595(0.9986)$, $E_1 = 1.990768(1.9901)$, $E_2 = 2.956244(2.9563)$. The same algorithm is then employed to evolve $\psi(x, y, t = 0)$ in real time under the HH potential in intense laser fields. In other words, TDSE is now solved in real time instead of solving a diffusion equation.

The parameters for the present calculation are:

Laser wavelength and frequency, $\lambda_{\rm L} = 1064$ nm, $\omega_{\rm L} = 0.0428228$ a.u.

Laser intensity $I = 5 \times 10^{13}$–2.001×10^{17} W cm^{-2}, $\Delta t = 0.05$.

$-150 \le x \le 150$, $-15 \le y \le 15$ for $I = 2 \times 10^{17}$, 2.001×10^{17} W cm^{-2}.

$-15 \le x \le 15$, $-5 \le y \le 5$ for $I = 5 \times 10^{13}$–1×10^{17} W cm^{-2}.

$\Delta x = \Delta y = 0.1$ for $I = 2 \times 10^{17}$, 2.001×10^{17} W cm^{-2}.

$\Delta x = \Delta y = 0.02$ for $I = 5 \times 10^{13} - 1 \times 10^{17}$ W cm^{-2}.

$0 \le t \le 2252.75$ (55 fs), 15 optical cycles.

For $I = 5\times10^{13}$–1×10^{17} W cm^{-2} the computations were carried out for 29 optical cycles. Since no noticeable difference was observed compared to 15 optical cycles, all the results are reported here up to 15 optical cycles. The linear ramp is $f(t) = t/t_0$ up to five optical cycles and unity thereafter. For the two highest intensities, a larger grid (specified above) was employed in order to take care of reflection/transmission of the wave function at/through the grid boundaries. Nevertheless, for these two intensities, the norm $N(t)$ changed by $\pm3\%$ and these fluctuations were taken care of by renormalizing the wave function to the last stable value (1.000267). Such fluctuations are characteristic of systems undergoing transitions to highly excited states, including the continuum, such that the probability density spreads over a large domain of space and therefore cannot remain confined within a computation grid. For comparison, we also report a similar study on an electron moving in a two-dimensional harmonic oscillator (HO) potential under a laser field of intensity 2×10^{17} W cm^{-2}.

The two different initial inputs (§1) generated in two different ways are:

(i) The ground state eigenfunctions $\psi_1(x, y, t = 0)$ and $\psi_2(x, y, t = 0)$ obtained with energy tolerance limits 10^{-12} and 10^{-8} respectively.

(ii) The wave function $\psi_1(x, y, t = 0)$ evolved under the HH potential in laser fields of slightly different intensities, i.e. 2×10^{17} and 2.001×10^{17} W cm^{-2}. When $\psi_1(x, y, t = 0)$ is evolved in time under the laser field of $I = 2.001 \times 10^{17}$ W cm^{-2}, it is designated as $\psi_1'(x, y, t)$.

It may be noted that the present methodology of numerically solving the TDSE should yield more accurate results than a Floquet-type analysis which may experience convergence problems under intense laser fields. Furthermore, these numerical solutions are basis-set-independent and are exact, in principle. Although an apparent disadvantage of these calculations is that they do not permit the use of symmetry-adapted basis sets, it may be noted that it is difficult to employ time-independent symmetry principles within a strong time-dependent perturbation such as intense laser fields because most of the time during interaction the potential function has no symmetry except when the field vanishes at $t = n\pi/\omega_{\mathrm{L}}$, $n = 0, 1, 2, \ldots$ [26] (see potential plots given later).

3. Results and discussion

Since both classical and quantum chaos are dynamical phenomena, we examine below various time-dependent quantities which might serve as signatures of quantum chaos for the electron moving in the HH potential under intense laser fields.

The correlation of the system with its initial state is measured in terms of the autocorrelation function [8]

$$C(t) = |\langle \psi_1(x, y, t = 0) | \psi_1(x, y, t) \rangle|^2. \tag{4}$$

Figure 1 shows the variation of $C(t)$ with time; the laser electric field $\varepsilon(t)$ is given in figure 1a. For the HH potential under low intensity (5×10^{13}–5×10^{16} W cm^{-2}, figures 1c and d) and the HO potential under intensity 2×10^{17} W cm^{-2} (figure 1a), the periodicity in $C(t)$ is twice that of $\varepsilon(t)$. Although the value of $C(t)$ falls below unity after five optical cycles, it periodically returns to its initial value. Thus, in all the three cases the system is well-correlated to its initial state. However, note that the fall in the value of $C(t)$ increases as the laser intensity is increased. But, when the HH potential is under the intensity 2×10^{17} W cm^{-2}, $C(t)$ decays rapidly and does not return to its starting value of unity. This behaviour indicates that the electron loses correlation with its initial quantum state under such a laser intensity and therefore this may be regarded as a signature of quantum chaos. In contrast, at zero field, $C(t)$ for the HH potential is unity for all times (figure 1e).

A similar behaviour is reflected in the power spectra $A(\omega)$ obtained through the fast Fourier transform (FFT) of $C(t)$ for the last six optical cycles with integration limits $t_1 = 819.15$ to $t_2 = 1638.35$. $A(\omega)$ is given by

$$A(\omega) = \left| \int_{t_1}^{t_2} C(t) \mathrm{e}^{-i\omega t} \mathrm{d}t \right|^2; \quad -\infty \leq \omega \leq +\infty, \quad C(t) = C(-t). \tag{5}$$

A relatively simple spectrum with a few lines is obtained for the HH potential at $I = 5 \times 10^{16}$ W cm^{-2} (figure 2c) and for the HO at $I = 2 \times 10^{17}$ W cm^{-2} (figure 2a).

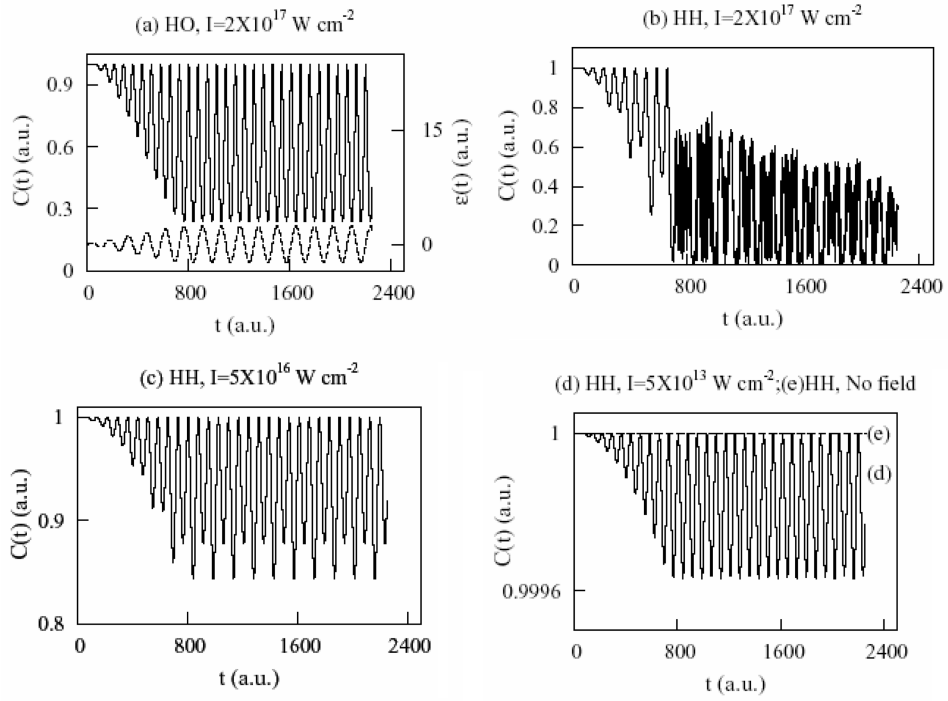

Figure 1. Plots of autocorrelation function $C(t)$ against time t in a.u. for (**a**) two-dimensional harmonic oscillator (HO) at $I = 2 \times 10^{17}$ W cm^{-2} and the Henon–Heiles (HH) oscillator at (**b**) $I = 2 \times 10^{17}$, (**c**) $I = 5 \times 10^{16}$, (**d**) $I = 5 \times 10^{13}$ W cm^{-2} respectively. As shown in (**e**), $C(t)$ for the HH oscillator at zero-field is just a horizontal line at unity. In (**a**) the laser electric field $\varepsilon(t)$ is shown in dotted line for $I = 2 \times 10^{17}$ W cm^{-2}. For other lower intensities the field amplitude decreases but the periodicity remains the same.

The HH potential at $I = 2 \times 10^{17}$ W cm^{-2} shows a rich spectrum (figure 2d) that has some characteristics of an atomic ATI spectrum as the higher energy peaks are less intense than the lower ones. However, at zero field, only the ground and first excited states are seen for the HH potential (figure 2b). The complete spectrum of energy levels of the HH potential below the dissociation energy (13.3333) is given in [14]. The comparative analysis of power spectrum obtained for HH at $I = 2 \times 10^{17}$ W cm^{-2} with the available energy spectrum reveals that about 25 states appear in the power spectrum with significant intensity. Higher excited states and the peak corresponding to the last bound state also appear, although with much less intensity. This implies that the continuum states are contributing to the power spectrum.

Figure 3 depicts the variation of the distance function [36,37] with time. Since the present work employs initial inputs generated in two different ways, $D(t)$ is defined separately for each initial input:

(i) Distance function obtained from slightly different initial wave functions $\psi_1(x, y, t = 0)$ and $\psi_2(x, y, t = 0)$ that are evolved under the same Hamiltonian

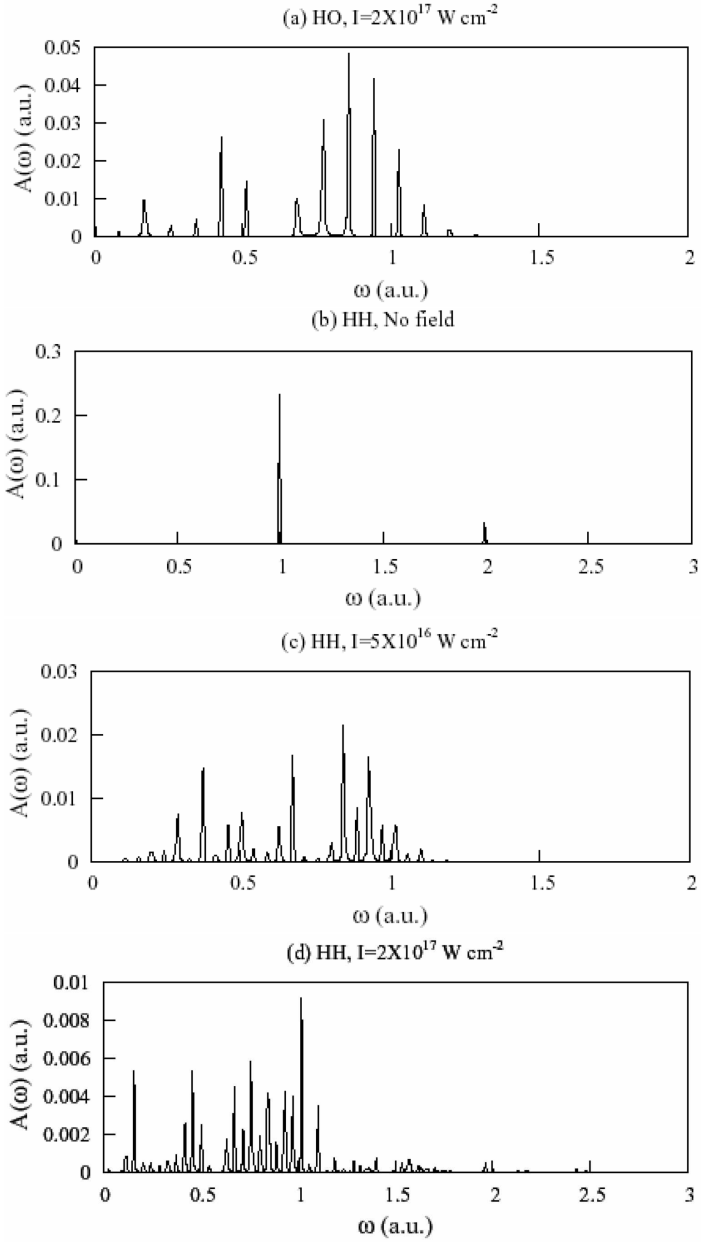

Figure 2. Power spectra plotted against the photon energy (ω), in a.u. for (**a**) the two-dimensional harmonic oscillator at $I = 2 \times 10^{17}$ W cm^{-2} and the Henon–Heiles oscillator at (**b**) zero field, (**c**) $I = 5 \times 10^{16}$, (**d**) $I = 2 \times 10^{17}$ W cm^{-2} respectively.

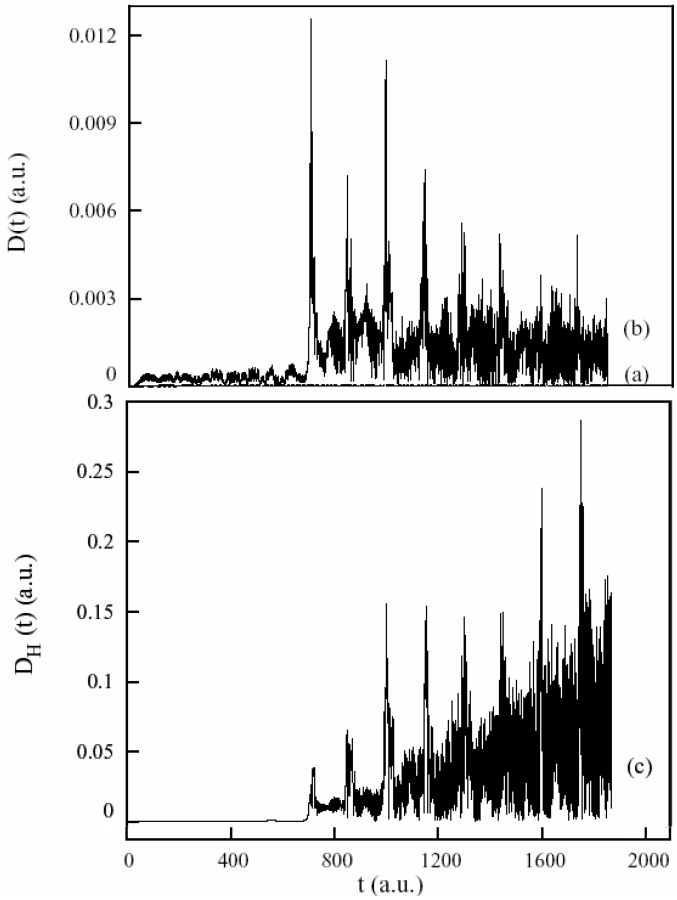

Figure 3. Plot of distance function $D(t)$, in a.u. of Henon–Heiles oscillator against time. Both (**a**), (**b**) refer to $D(t)$ calculated with two slightly different initial states and (**c**) refers to $D_{\mathrm{H}}(t)$ calculated with two slightly different Hamiltonians. (**a**) $I = 0.0$, 5×10^{13}–1×10^{17}, (**b**) $I = 2 \times 10^{17}$ and (**c**) $I = 2.001 \times 10^{17}$ W cm^{-2} respectively.

is given by

$$D(t) = \{(\langle x_1(t)\rangle - \langle x_2(t)\rangle)^2 + (\langle p_{x_1}(t)\rangle - \langle p_{x_2}(t)\rangle)^2\}^{1/2}, \tag{6}$$

where $\langle x_1(t)\rangle$, $\langle p_{x_1}(t)\rangle$, $\langle x_2(t)\rangle$ and $\langle p_{x_2}(t)\rangle$ are expectation values at time t of position and momentum operators in the x-direction with respect to $\psi_1(x, y, t)$ and $\psi_2(x, y, t)$ respectively. Here expectation values in the y-direction, i.e., $\langle y\rangle$ and $\langle p_y\rangle$ are not considered since the potential is symmetric in the y-direction and therefore these values vanish, as verified computationally for further checking the numerical accuracy of our method.

(ii) Distance function obtained from the same initial wave function that is evolved under slightly different Hamiltonians is given by

$$D_{\mathrm{H}}(t) = \{(\langle x_1(t)\rangle - \langle x_1'(t)\rangle)^2 + (\langle p_{x_1}(t)\rangle - \langle p_{x_1}'(t)\rangle)^2\}^{1/2}. \tag{7}$$

Here $\langle x_1'(t)\rangle$ and $\langle p_{x_1}'(t)\rangle$ are expectation values calculated with $\psi_1'(x, y, t)$. Note that $\psi_1(x, y, t = 0) = \psi_1'(x, y, t = 0)$. Figure 3a shows minor fluctuations in $D(t)$ that fall on a straight line for HH at $I = 5 \times 10^{13}$–1×10^{17} W cm^{-2} and HO for the laser intensity 2×10^{17} W cm^{-2}. The zero-field case of the HH potential also falls on a straight line (figure 3a). When the HH potential is under the intensity 2×10^{17} W cm^{-2}, there are prominent peaks after 5 optical cycles (figure 3b). But the change in $D(t)$ is negligible as compared to the increase in $D_{\mathrm{H}}(t)$ (figure 3c). Also, the peak height decreases in $D(t)$ whereas it increases for $D_{\mathrm{H}}(t)$. Thus, the distance corresponding to two identical wave functions that are evolving in quantum 'phase-space' (see later) under slightly different Hamiltonians increases. This is analogous to the exponential divergence of classical phase-space trajectories characteristic of chaotic systems. This behaviour also exhibits greater sensitivity of quantum motion to small changes in the Hamiltonian rather than in the initial quantum state when the underlying classical motion is chaotic.

Another criterion to measure the sensitivity of quantum dynamical motion to the initial quantum state or the Hamiltonian is provided by the overlap integral, $I(t)$ [28]. For the slightly different initial wave functions, $\psi_1(x, y, t = 0)$ and $\psi_2(x, y, t = 0)$ that are evolved under the same Hamiltonian, $I(t)$ is given by

$$I_1(t) = |\langle\psi_1(x, y, t)|\psi_2(x, y, t)\rangle| \tag{8}$$

and when $\psi_1(x, y, t = 0)$ and $\psi_1'(x, y, t = 0)$ ($\psi_1 = \psi_1'$, only at $t = 0$) are evolved under slightly different Hamiltonians, $I(t)$ is defined as

$$I_2(t) = |\langle\psi_1(x, y, t)|\psi_1'(x, y, t)\rangle|. \tag{9}$$

In view of the fact that the quantum time-evolution operator is unitary, $I_1(t)$ should remain constant in time at any particular laser intensity. Figure 4a shows that $I_1(t)$ maintains a steady initial value of unity whereas figure 4b shows that, starting from an initial value of unity, $I_2(t)$ decays rapidly after five optical cycles and falls to 0.72 at the end of the 15th optical cycle. The constancy of $I_1(t)$ in time is a further check on the numerical accuracy of our algorithm. Thus, the decay of the overlap between the time-evolved quantum states under slightly different Hamiltonians again exhibits greater sensitivity of quantum motion to slight changes in the Hamiltonian.

It is worthwhile to note that $I_2^2(t)$ may be identified as the quantum fidelity or Loschmidt echo [28–32] except that both $\psi_1(x, y, t)$ and $\psi_1'(x, y, t)$ refer to perturbed states. However, if one considers $\psi_1(x, y, t)$ as originating from an 'unperturbed' Hamiltonian that incorporates the original oscillator potential plus the laser potential, and looks upon $\psi_1'(x, y, t)$ as originating from a 'perturbed' Hamiltonian in which the laser intensity is slightly changed, then $I_2^2(t)$ indeed becomes the fidelity (note that since our classical system of reference is the oscillator in the absence of a laser field, we do not adopt such a viewpoint here). It is known that fidelity decay can be taken as a reliable indicator of quantum chaos in the unperturbed system provided the applied perturbation commutes with a classical coordinate [30]. From eq. (2), it is clear that this condition is satisfied for the present system. For systems exhibiting classical chaos, fidelity decay was found to be Gaussian or exponential,

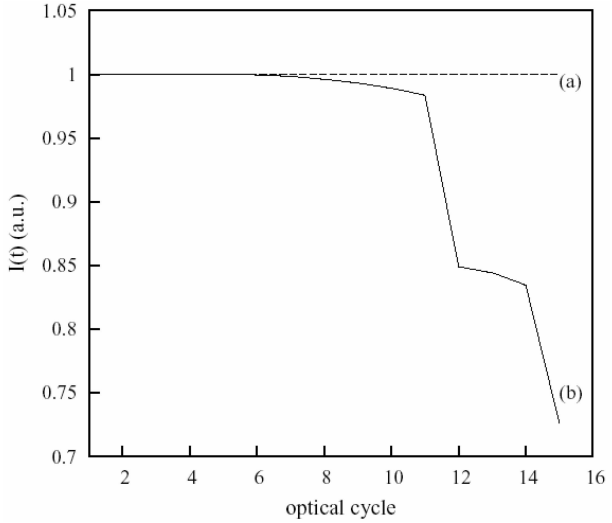

Figure 4. Overlap integral $I(t)$ plotted in a.u. against optical cycle. (**a**) refers to $I_1(t)$ calculated with two slightly different initial states while (**b**) refers to $I_2(t)$ obtained for slightly different Hamiltonians.

including a Lyapunov regime [32]. Since this was not considered satisfactory, Wang *et al* [32] have proposed a general semiclassical approach to fidelity decay in the limit of large perturbations. In the present case, we have studied the decay of $I_2(t)$ from unity in course of time.

The variation of quantum 'phase-space' volume [8] $V(t)$, or the uncertainty product, with time and the laser electric field $\varepsilon(t)$ are given in figure 5. $V(t)$ is defined as

$$V(t) = \{(\langle x^2\rangle - \langle x\rangle^2)(\langle p_x^2\rangle - \langle p_x\rangle^2)\langle y^2\rangle\langle p_y^2\rangle\}^{1/2}, \tag{10}$$

where all the expectation values are with respect to $\psi_1(x, y, t)$. $V(t)$ remains nearly constant for the HH potential under lower field intensities ($I = 5 \times 10^{13}$–1×10^{17} W cm^{-2}, figure 5b) and for the HO potential under $I = 2 \times 10^{17}$ W cm^{-2} (figure 5b). The HH potential at zero field also falls on (b). $V(t)$ increases after five optical cycles and is around 1800 for the HH potential at $I = 2 \times 10^{17}$ W cm^{-2}. Interestingly, the maxima in $V(t)$ correspond to the minima in the laser electric field $\varepsilon(t)$. A large increase in $V(t)$ can be interpreted as the fingerprint of quantum chaos as it implies a loss of information about the electron being represented by the wave packet. Note that while excitation to the continuum might increase $V(t)$ for a non-quantum-chaotic system, the nature and magnitude of such increase should be qualitatively different for a quantum chaotic system. It may also happen that after an initial increase, $V(t)$ no longer increases significantly, leading to a partial suppression of quantum chaos [38]. This, however, did not happen in the present case.

There is a likelihood of the system characterized by large $V(t)$ to follow a chaotic trajectory. Figure 6 shows the quantum 'phase-space' trajectories where $\langle x(t)\rangle$ is plotted against $\langle p_x(t)\rangle$ in the spirit of Ehrenfest theorem. Figures 6a, c, and d show

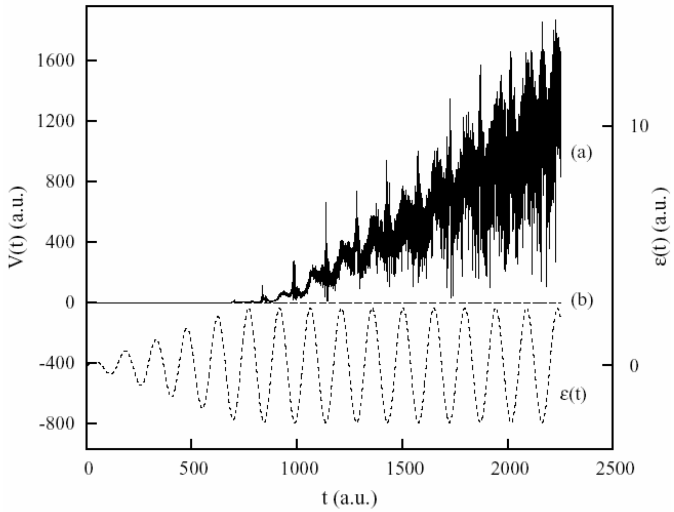

Figure 5. Plot of 'phase-space' volume of Henon–Heiles oscillator against time. (**a**) refers to $I = 2 \times 10^{17}$ W cm^{-2} while (**b**) refers to $I = 0.0$, 5×10^{13}–1×10^{17} W cm^{-2} as well as the two-dimensional harmonic oscillator at $I = 2 \times 10^{17}$ W cm^{-2}. The laser electric field $\varepsilon(t)$ is also shown in dotted line. All quantities are in atomic units.

the spiral trajectory obtained for the HH potential in laser fields of lower intensities and for the HO potential at $I = 2 \times 10^{17}$ W cm^{-2}. When the HH potential is under the laser field of this intensity, the trajectory starts as a spiral but rapidly diverges into a complicated pattern (figure 6b). For the zero-field case of the HH potential, the trajectory is again a spiral (figure 6e) which is more like a quashed spring in which every turn is displaced from the previous one due to a kink in the turn (figure 6f). When the laser field is switched on, the displacements of the turns in the spring diminish as the laser intensity increases, until the trajectory becomes chaotic at the highest intensity.

It may be mentioned here that the trajectories obtained by evolving slightly different wave functions under the same Hamiltonian superimpose on each other. This indicates that the time-evolution of quantum systems is much more sensitive to small changes in the Hamiltonian, than to small changes in the initial ground state. This is in accord with earlier studies [28,29] which demonstrated that the evolution of a quantum state was altered under a slightly perturbed (small internal perturbation) Hamiltonian, the overlap between the perturbed and unperturbed states tended to a comparatively smaller value if the analogous classical motion is chaotic than if it is regular. This may be explained by saying that in quantum dynamical motion all the states are mixed (linear combination of other states), whereas the classical exponential sensitivity to the initial state applies only to an individual state [18]. However, it has also been argued that quantum systems exhibit a state sensitivity very similar to classical state sensitivity, by using computational motion reversal [18]. Note that in the present case, due to strong perturbation, the fall in $I_2(t)$ with time is quite significant (nearly 30%).

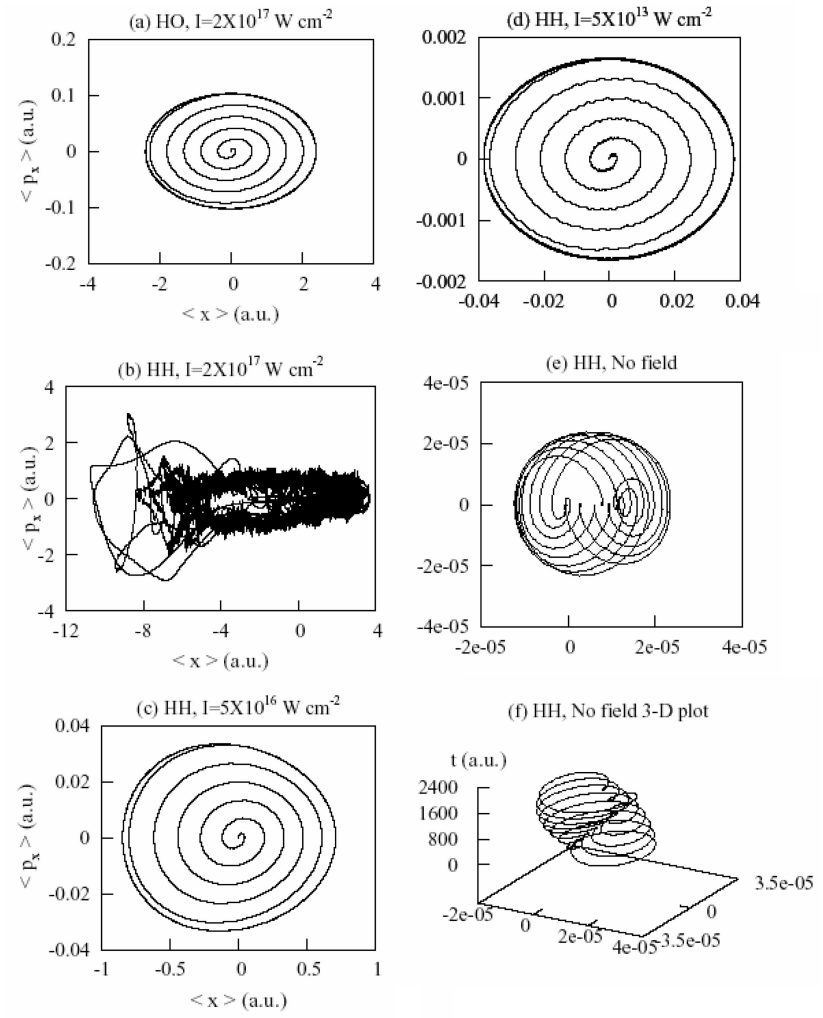

Figure 6. Quantum 'phase-space' trajectories, in a.u., of (**a**) the two-dimensional harmonic oscillator at $I = 2 \times 10^{17}$ W cm^{-2} and of the Henon–Heiles oscillator at (**b**) $I = 2 \times 10^{17}$, (**c**) $I = 5 \times 10^{16}$, (**d**) $I = 5 \times 10^{13}$ W cm^{-2} respectively, and (**e**) zero-field (with the same axial system). In (**f**), a three-dimensional plot of the zero-field case (**e**) is shown with the x-axis as $\langle x \rangle$, y-axis as $\langle p_x \rangle$ and z-axis as time (a.u.) For (**a**)–(**d**), Δt between successive contours is 0.05 a.u. while it is 6.5 a.u. for (**e**) and (**f**).

Figure 7 shows $\langle p_x(t) \rangle$ for HH at $I = 2 \times 10^{17}$ W cm^{-2} against $\langle x(t) \rangle$ at the end of each optical cycle. The values lie close together for the first few optical cycles but diverge by the end of the 15th optical cycle, thus displaying greater sensitivity to the initial Hamiltonian.

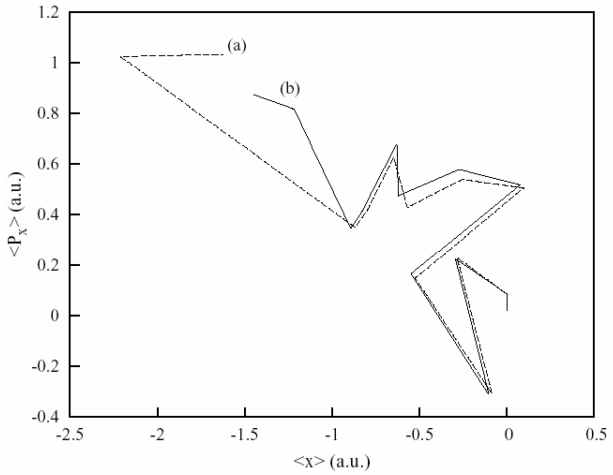

Figure 7. The expectation values (a.u) $\langle p_x(t)\rangle$ of the momentum operator in x-direction, plotted against the expectation value of position operator $\langle x(t)\rangle$ at the end of each optical cycle, for the Henon–Heiles oscillator. (**a**) $I = 2.001 \times 10^{17}$, (**b**) $I = 2 \times 10^{17}$ W cm^{-2}.

The potential energy surfaces (PES) and the probability densities at $t = 0$ as well as at the crest ($\varepsilon_0 = 2.387202$, $t = 2090.85$) and trough ($\varepsilon_0 = -2.387202$, $t = 2164.20$) of the 15th optical cycle are shown in figure 8. The ground-state probability density is given by a single centrosymmetric peak (figure 8d). The shifting of the minima of the PES and likewise the spread of probability density is in the positive and negative x-direction respectively at the crest (figures 8b and 8e) and at the trough (figures 8c and 8f) of the laser electric field. It is clear that the initial quantum state is evolving into a mixture of numerous states. When the HH potential is under a low-intensity field, the norm was preserved at unity but it is changed by $\pm 3\%$ when the applied laser intensity is 2×10^{17} W cm^{-2}, even though a larger grid was employed at this intensity. This indicates that the probability density is leaking into the continuum. Moreover, the spread of the probability density all over the grid and the existence of higher bound states in the power spectrum suggest that an electron moving under the HH potential in the presence of a laser field of intensity 2×10^{17} W cm^{-2} has reached the continuum. This is further supported by the HHG spectrum $H(\omega)$ obtained by taking the FFT of the time-varying dipole moment, $\mu(t) = \langle \psi_1(x, y, t)|x|\psi_1(x, y, t)\rangle$. $H(\omega)$ is calculated for the last six optical cycles with integration limits $t_1 = 819.15$ to $t_2 = 1638.35$, viz.,

$$H(\omega) = \left| \int_{t_1}^{t_2} \mu(t) \mathrm{e}^{-i\omega t} \mathrm{d}t \right|^2; \quad -\infty \leq \omega \leq +\infty, \quad \mu(t) = \mu(-t) \tag{11}$$

and plotted against the harmonic order. There is no significant harmonic spectrum below 2×10^{17} W cm^{-2} as the electron has not reached the highly excited states (figures 9c, d). For the HO (figure 9a), the spectrum shows a single peak as it is a bound potential. The plateau of harmonics obtained in the HHG spectrum at

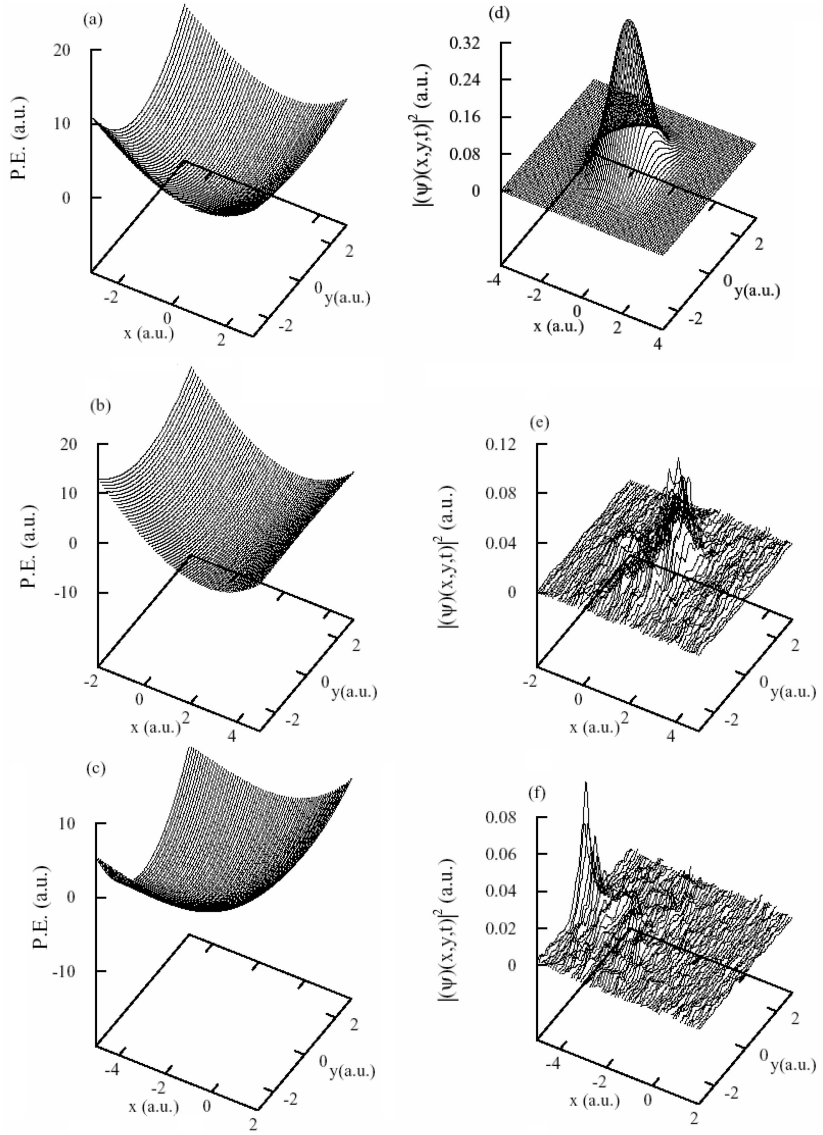

Figure 8. The Henon–Heiles oscillator potential energy surfaces (**a**,**b**,**c**) and the corresponding probability densities (**d**,**e**,**f**) in a.u., for $I = 2 \times 10^{17}$ W cm^{-2}. (**a**), (**d**) correspond to $t = 0$ while (**b**), (**c**) correspond to the crest ($\varepsilon(t) = \varepsilon_0$, $t = 2090.5$ a.u.) and (**c**), (**f**) correspond to the trough ($\varepsilon(t) = -\varepsilon_0$, $t = 2164.20$ a.u.) respectively of the 15th optical cycle.

$I = 2 \times 10^{17}$ W cm^{-2} results from transitions to the continuum and subsequent emissions to lower levels, especially the ground state. The spectrum has a rich multiplet structure that is rich in both even and odd harmonics (inset of figure 9b).

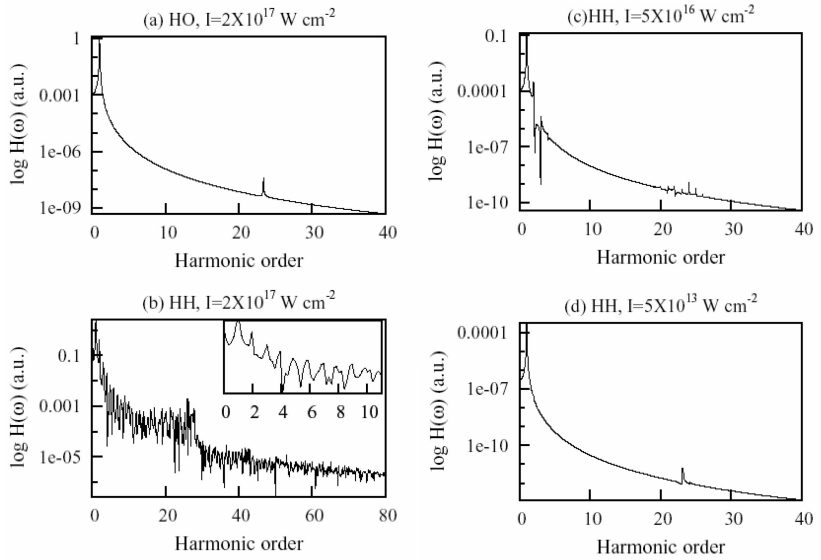

Figure 9. HHG spectrum in a.u. is plotted against harmonic order ($\omega/\omega_{\rm L}$) for (**a**) the two-dimensional harmonic oscillator at $I = 2 \times 10^{17}$ W cm^{-2} and the Henon–Heiles oscillator at (**b**) $I = 2 \times 10^{17}$, (**c**) $I = 5 \times 10^{16}$, (**d**) $I = 5 \times 10^{13}$ W cm^{-2} respectively. The inset of (**b**) shows both even and odd harmonics. (**c**) shows only the 1st and 2nd harmonics while (**d**) shows only the first harmonic.

Interestingly, it has the characteristic features of HHG spectra of atoms and molecules, viz., a rapid initial decrease in signal intensity followed by a plateau followed by a sharp fall in intensity. Thus, the parallelism between nonlinear oscillators and atoms/molecules regarding their interactions with intense laser fields [26] is further reinforced.

4. Conclusion

The present work confirms the two speculations made in §1 as follows:

1. When a classically chaotic system such as an electron moving under the HH potential is lifted to the quantum continuum by a strong periodic driving force such as that from intense laser fields, it exhibits quantum chaos. However, in order to reach the continuum, a threshold laser intensity (2×10^{17} W cm^{-2} in the present case) is required below which quantum chaos is not manifested even in a nonintegrable system like the HHO. Note that atoms and molecules also require a threshold intensity in order to reach the quantum continuum and display characteristic features of matter-intense-laser interactions such as ATI, HHG, etc. At the threshold intensity, various dynamical (time-dependent) signatures of quantum chaos such as (i) the lack of correlation with the initial state, (ii) increase in the distance function, (iii) decrease in the overlap integral, (iv) increase in the quantum 'phase-space' volume, and (v)

divergence of trajectories in the quantum 'phase-space' have been examined. The system's incursion into the quantum continuum has been demonstrated through the ATI-like power spectrum, HHG spectrum and probability density plots. Note that the two-dimensional quantum harmonic oscillator does not display quantum chaos irrespective of the laser intensity, because there is no continuum or 'pseudocontinuum' (see ref. [26] for the explanation of 'pseudocontinuum').

The present approach characterizes quantum chaos as sensitivity to the initial quantum state, in the same spirit as in classical (deterministic) chaos. However, in view of the unitarity of the time-evolution operator, the sensitivity is not towards an initial 'pure' quantum state (a single eigenstate) but towards an initial state characterized by a mixture of quantum states. This mixture or wave packet is created by the time-dependent perturbation itself acting on a single eigenstate at $t = 0$. Two slightly different initial mixtures of quantum states have been created at the end of the first time step (0.05 a.u.) by small changes in the laser intensity, i.e. the Hamiltonian. While sensitivity to small changes in the Hamiltonian have been observed before, in the absence of any external perturbation [18,34], to the best of our knowledge, the results and insights presented in this work by bringing a strong, external time-dependent perturbation and the quantum continuum into consideration, have not been reported before. It may also be noted that while some of the signatures of quantum chaos, examined in this paper, have been employed separately by other workers, our conclusions on quantum chaos have been guided by a combination of all the dynamical (time-dependent) signatures rather than any individual signature.

2. Like one-dimensional nonlinear oscillators [26], two-dimensional coupled nonlinear oscillators are suitable model systems for studying laser–matter interactions as they mimic the behaviour of atoms/molecules in intense laser fields, e.g., in the ATI-like spectra, HHG spectra, stabilization in superintense laser fields, etc. The decade-old conjecture [25] that atoms, e.g., the He atom, should exhibit quantum chaos under intense laser fields is thus verified through the parallel system of a coupled two-dimensional nonlinear oscillator. It also raises the interesting possibility of classically integrable systems, with quantum continua of their own, exhibiting quantum chaos on excitation to the continuum by an intense laser field. Furthermore, in case the HH potential is experimentally realized for electronic motion, it would provide a relatively simple way to generate X-ray lasers and attosecond lasers (see, e.g., [26,39]).

Acknowledgement

BMD thanks N Moiseyev for discussion. NG gratefully acknowledges financial support from the Council of Scientific and Industrial Research (CSIR), New Delhi.

References

[1] M C Gutzwiller, *Chaos in classical and quantum mechanics* (Springer, Berlin, 1990)

[2] G Casati, B V Chirikov, F M Izrailev and J Ford, in *Stochastic behaviour in classical and quantum Hamiltonian systems* edited by G Casati and J Ford (Springer-Verlag, New York, 1979)
[3] N Pomphrey, *J. Phys.* **B7**, 1909 (1974)
[4] D W Noid, M L Koszykowski and R A Marcus, *J. Chem. Phys.* **71**, 2864 (1979)
[5] K S J Nordholm and S A Rice, *J. Chem. Phys.* **61**, 203 (1974)
[6] M J Davis and E J Heller, *J. Chem. Phys.* **75**, 3916 (1981)
[7] J S Hutchinson and R E Wyatt, *Phys. Rev.* **A23**, 567 (1981)
[8] M D Feit and J A Fleck Jr., *J. Chem. Phys.* **80**, 2578 (1984)
[9] P Brumer and M Shapiro, *Chem. Phys. Lett.* **72**, 528 (1980)
[10] P K Chattaraj and S Sengupta, *Phys. Lett.* **A181**, 225 (1993)
[11] P K Chattaraj and S Sengupta, *Ind. J. Pure Appl. Phys.* **34**, 518 (1996)
[12] P K Chattaraj, S Sengupta and A Poddar, *Curr. Sci.* **74**, 758 (1998)
[13] D W Noid, M L Koszykowski, M Tabor and R A Marcus, *J. Chem. Phys.* **72**, 6169 (1980)
[14] M D Feit, J A Fleck, Jr. and A Steiger, *J. Comp. Phys.* **47**, 412 (1982)
[15] G Benettin, C Froeschle and J P Scheidecker, *Phys. Rev.* **A19**, 2454 (1979)
[16] A Kolmogorov, *Dokl. Akad. Nauk. SSSR* **124**, 774 (1959)
[17] Ya Sinai, *Izv. Akad. Nauk SSSR Ser. Mat.* **25**, 899 (1961)
[18] L E Ballentine and J P Zibin, *Phys. Rev.* **A54**, 3813 (1996)
[19] M Gavrila (ed.), *Atoms in intense laser fields* (Academic Press, New York, 1992)
[20] M H Mittleman, *Introduction to the theory of laser–atom interactions* (Plenum Press, New York, 1993)
[21] A D Bandrauk (ed.), *Molecules in laser fields* (Marcel Dekker, New York, 1994)
[22] K Burnett, V C Reed and P L Knight, *J. Phys.* **B26**, 561 (1993)
[23] M Protopapas, C H Keitel and P L Knight, *Rep. Progr. Phys.* **60**, 389 (1997)
[24] H Eberly and K C Kulander, *Science* **262**, 1229 (1993)
[25] B Kr Dey and B M Deb, *Int. J. Quant. Chem.* **56**, 707 (1995)
[26] A Wadehra, Vikas and B M Deb, *J. Chem. Phys.* **119**, 6620 (2003) and other references therein
[27] A Wadehra and B M Deb, *Proc. Indian Acad. Sci. Chem. Sci.* (C N R Rao Festschift), **115**, 349 (2003); Erratum: *J. Chem. Sci.* **116**, 129 (2004)
[28] A Peres, *Phys. Rev.* **A30**, 1610 (1984)
[29] A Peres, *Quantum theory*: *Concepts and methods* (Kluwer, Dordrecht, 1993) Chap. 11
[30] J Emerson, Y S Weinstein, S Lloyd and D G Cory, *Phys. Rev. Lett.* **89**, 284102 (2002)
[31] G Benenti, G Casati and G Veble, *Phys. Rev.* **E68**, 036212 (2003)
[32] W Wang, G Casati, B Li and T Prosen, *Phys. Rev.* **E71**, 037202 (2005)
[33] B L Hammond, W A Lester and P J Reynolds, *Monte Carlo methods in ab initio quantum chemistry* (World Scientific, Singapore, 1994)
[34] A K Roy, N Gupta and B M Deb, *Phys. Rev.* **A65**, 012109 (2002)
[35] A Wadehra, A K Roy and B M Deb, *Int. J. Quant. Chem.* **91**, 597 (2003)
[36] U Schwengelbeck and F H M Faisal, *Phys. Lett.* **A199**, 281 (1995)
[37] F H M Faisal and U Schwengelbeck, *Phys. Lett.* **A207**, 31 (1995)
[38] N Gupta and B M Deb, *Chem. Phys.* **327**, 351 (2006)
[39] Y Mairesse, A de Bohan, L J Frasinski, H Merdji, L C Dinu, P Monchicourt, P Breger, M Kovacev, R Taieb, B Carre, H G Muller, P Agostini and P Salieres, *Science* **302**, 1540 (2003)